ORIGINAL RESEARCH

Comparative analysis of European vertical landing reusable first stage concepts

Jascha Wilken[1] · Sven Stappert[1]

Abstract

Reusable launch systems have the potential to significantly impact the space launch service market if both a high reliability and low refurbishment costs can be achieved. This study delves into the Vertical Takeoff and Vertical Landing (VTVL) methodology, as currently employed by SpaceX, and forms a segment of the ENTRAIN study by DLR. This broader study encompasses an examination of both Vertical Takeoff Horizontal Landing (VTHL) and VTVL reusable first stages, exploring their performance across high-level design parameters. This manuscript's primary objective is to assess the quantitative impact of high-level design factors on launch vehicle performance, particularly in relation to the development of a future European reusable launch system featuring a VTVL first stage. For a two-stage vehicle with a payload performance of 7.5t into GTO, the effect of varying propellant combinations, staging velocities and engine cycles are assessed. The study encompasses an iterative, multidisciplinary analysis and sizing process for ten different configurations. Each design iteration not only entails a structural design analysis but also includes optimization of the ascent and descent trajectories. Finally, the developed vehicle concepts are compared to derive quantitative insights into the trade-offs associated with key design choices.

Keywords Reusable launch vehicle · VTVL · Multidisciplinary analysis

1 Introduction

As the Ariane 6 nears completion, the future trajectory of launcher development in Europe remains unclear. It currently appears likely that the next large launcher will be partially reusable. Yet, other aspects of the architecture were unclear when this study was initiated in 2018 and continue to be undefined. This includes critical aspects such as the vehicle staging, the fuel selection and the engine cycle. Although qualitative arguments for various choices are well-established, their quantitative impact on the overall vehicle system is less clear. For example, it is known that hydrogen offers extremely high performance with regard to the specific impulse but comes with the challenges associated with extremely low boiling temperature and low density. In contrast, hydrocarbon fuels, though denser, are associated with lower specific impulses.

The resulting quantitated effect of these conflicting qualitative trends on launcher performance is not well established and may differ significantly across various use cases. Accurately determining this impact requires a comprehensive, multidisciplinary evaluation of the entire launcher system for each considered option.

Multidisciplinary Design Optimization (MDO) for Vertical Takeoff and Vertical Landing (VTVL) first stages using various propellant combinations is established in current literature [1, 2]. However, these studies simplify subdiscipline models to facilitate actual optimization without excessive computational costs. For instance, rather than simulating ascent and descent trajectories, Δv budgets are typically used to assess launcher performance.

In contrast, studies with more detailed subdiscipline modeling usually focus on a limited selection of reference vehicles. The RETALT project [3], for example, conducted an in-depth investigation of two reference VTVL vehicles, particularly in terms of technologies required for the propulsive return of the stage.

Older system studies like FESTIP [4] that compared different options for European reusable vehicles only considered a hydrogen-fueled VTVL Single Stage to Orbit (SSTO).

✉ Jascha Wilken
jascha.wilken@dlr.de

1 Deutsches Zentrum für Luft- und Raumfahrt, System Analysis for Space Transportation, Institute for Space Systems, Bremen, Germany

 Springer

There exists a notable gap in published literature regarding the comparison of high-level design options based on a multidisciplinary design analysis, especially within the current European context.

The Europe's NexT Reusable ArIaNe (ENTRAIN) study by the DLR seeks to address this gap by quantitatively evaluating options for a partially reusable European launch system, laying a solid technical foundation for future discussions. While the extent of variations and iterations precludes the use of high-fidelity methods like Computational Fluid Dynamics (CFD) or Finite Element (FE) models, key sub-disciplines are modeled using specialized conceptual design tools. For example, the evaluation of each launcher in the study includes structural design analysis, optimization of both ascent and descent trajectories, and modeling of the propellant tank and associated feed, fill, and pressurization lines.

The study examines a range of design parameters, including staging velocity, fuel choice, engine cycle, and recovery method, to provide a comprehensive understanding of the trade-offs and potentials of various design choices.

The scope of the study is broad, and its findings are detailed in several publications. [5] provides an overview of the study's methodology and its relation to other European projects. [6] delves into propulsion datasets and the underlying rocket engine models. While this manuscript concentrates on the concepts employing a VTVL approach, the equivalent variants with the winged vehicles and horizontal landing are discussed in [7]. Finally, within [8] the different recovery approaches and compared in depth to each other.

While the study itself encompasses different recovery methods, this paper focusses on the modeling of launch vehicles employing the Downrange Landing (DRL) mode, first successfully used by SpaceX.

1.1 Study logic and high-level assumptions

The ENTRAIN study was structured into two parts: the first part concentrates on a comparative analysis of VTVL and VTHL launchers ensuring uniformity in the investigation level to prevent distortions from varied degrees of detail. Therefore, identical high-level requirements and assumptions are used for all return methods. This paper introduces the VTVL launchers investigated in this first part of the ENTRAIN study. They were all evaluated with regard to the following high-level requirements:

- 7000 kg + 500 kg margin payload to Geostationary Transfer Orbit (GTO) of 250 km × 35786 km × 6° (standard Ariane 5 GTO) via a LEO parking orbit of 140 km × 330 km × 6°, see sect. 2.6.1 for details
- launch from Centre Spatial Guyanais (CSG), Kourou
- Two Stage to Orbit (TSTO) configurations

- same propellant combination in both stages
- same engines in both stages with exception of different nozzle expansion ratios

In the launchers detailed in sect. 3, an exception to the aforementioned two requirements is included: a hybrid launcher configuration. This unique model incorporates a methane-fueled lower stage and a hydrogen-fueled upper stage. The feasibility, potential advantages, and limitations of this hybrid launcher are discussed in sect. 4.

Based on these requirements, the following degrees of freedom were explored:

- Engine Cycles: Gas Generator (GG) and Staged Combustion (SC);
- VTVL with retropropulsion landing on downrange barge (DRL) or with Return-to-Launch-Site (RTLS);
- 2nd stage Δv of 6.2 km/s, 6.6 km/s, 7.0 km/s, 7.6 km/s.
- propellant combinations:
- Liquid oxygen (LOX)/ Liquid hydrogen (LH2);
- LOX/Liquid methane (LCH4);
- LOX/Liquid propane (LC3H8);
- LOX/kerosene, Rocket Propellant-1 (RP-1).

In the analysis of the staging variations, the upper stage Δv was chosen instead of the more commonly used separation Mach number. This decision was made to decouple the staging parameter from the variances caused by separation different altitudes, where atmospheric properties such as speed of sound can vary significantly. These variations limit the comparability exclusively via Mach number. For reference, the upper stage Δv of 6.2 km/s, 6.6 km/s, 7.0 km/s, 7.6 km/s approximately correspond to a separation Mach numbers of 15, 12, 10 and 7, respectively.

A comprehensive staging optimization would require a reliable cost function, which for reusable stages will depend on the cost of recovery and refurbishment of a used stage. Given the substantial uncertainties surrounding refurbishment and the impact of the stage separation velocity on these costs a full optimization was deemed impractical. Instead this parametric approach was chosen for this study.

In a preliminary design phase of the ENTRAIN study, when sizing the various combinations SI curves, it was found that the configurations with an upper stage Δv of 6.2 or 7.6 km/s resulted in excessively heavy and impractical launchers. The same result was found when trying to meet the required GTO performance with a first stage returning via RTLS. Fulfilling the total Δv requirement of the RTLS maneuver and the demanding GTO mission with a TSTO vehicle leads to excessive vehicle sizes, especially for the hydrocarbon-fueled concepts. Consequently, these options were excluded from the more detailed design study shown

hereafter. The results of the preliminary design phase are described in [9].

2 Methods

2.1 Launcher architecture

As described in [5], it was assumed that all launchers will be TSTO vehicles. Most launchers described hereafter share the same general layout: The same propellant combination in both stages as well as the same engines for both stages, albeit with a larger nozzle on the second stage. This is considered cost effective since only one engine core has to be developed and the high number of engines on the first stage results in a higher production rate, thus reducing both development and production cost per unit.

During the study, one exception to this architecture was added: The possibility of a hydrogen-fueled upper stage and a methane-fueled first stage was also evaluated, even though it does not strictly adhere to the above-mentioned logic. Even though this combination was found to be very performant, the need for two engine developments and the handling of two propellants at the launch pad has to be considered. This exception is hereafter referred to as the hybrid launcher.

2.2 Sizing logic

The design of launch vehicles is inherently iterative due to the interdependence of various subsystems. For each launcher, the initial design variables were the propellant loadings for both stages. Once these were determined, the vehicle geometry could be derived, assuming a constant length-to-diameter ratio of ~ 15 for the entire launcher. With the geometry established, the aerodynamic coefficients can be estimated. Based on these inputs, the structural analysis, mass model, and trajectory optimization were addressed iteratively.

The main propulsion system was sized so that the thrust-to-weight (T/W) ratio at take-off was close to 1.4, with a number of engines that kept the T/W of the upper stage between 0.8 and 1.2.

The process then progressed to the optimization of ascent and descent trajectories to evaluate the total payload capacity and the Δv provided by the upper stage. The design of the launcher was considered to have converged once these values aligned closely with the targeted objectives, allowing for a margin of ± 150 kg for payload and ± 100 m/s for upper stage Δv. The sizing process used in this study is outlined in Fig. 1. The arrows to the left of a subsystem indicate the iterative loops necessary to achieve a convergent design.

2.3 Aerodynamic coefficients

The aerodynamic coefficients in this study were estimated using empirical methods similar to those in DATCOM [10], as implemented in the DLR tool cac [11]. With these methods, the aerodynamic properties of simple rotationally symmetric bodies with conic or ogive noses can be quickly assessed using analytical formulas supported by wind tunnel data.

While these methods are well suited for estimating coefficients for forward-flying launch vehicles, they do not inherently account for configurations like the engine-forward orientation during reentry. The complex geometry of the aft bay and multiple engine nozzles cannot be readily accounted for with cac. Therefore, for modeling the descent phase, the vehicle was represented within cac as a blunt cylinder. The

Fig. 1 Sketch of Launcher sizing process for ENTRAIN VTVL launch vehicles. The arrows to the left of a subsystem indicate the iterative loops necessary to achieve a convergent design
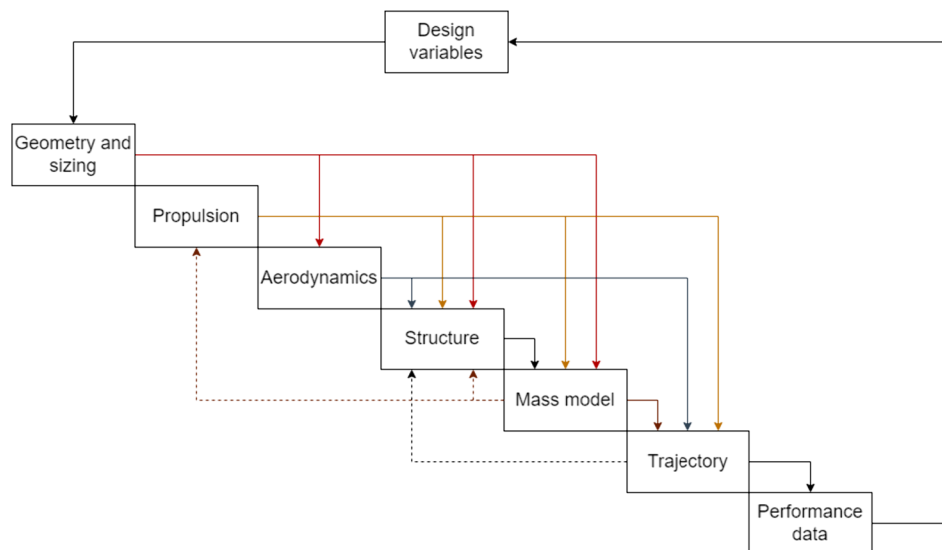
Fig. 2 Exemplary zero-lift drag coefficient used for both ascent and descent orientation, specifically for the CC GG Med configuration
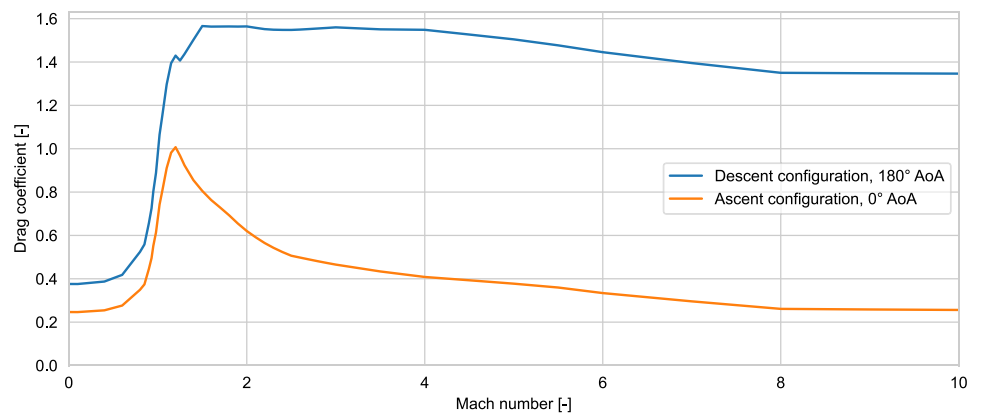

Table 1 LOX/RP-1, LOX/LC3H8, rocket engine data

Propellants	LOX/RP-1		LOX/LC3H8	
Case	1st stage	2nd stage	1st stage	2nd stage
Engine cycle	GG	GG	GG	GG
Expansion ratio	20	120	20	120
Sea level Isp [s]	279	–	284	–
Vacuum Isp [s]	310	338	315	344
Engine T/W [-]	113	90	111	88

aerodynamic coefficients obtained from this model were then scaled to align with wind tunnel data for the zero-lift drag coefficient of blunt cylinders [12]. This approach was retroactively corroborated in subsequent studies, where similar aerodynamic configurations were analyzed using CFD calculations [13].

As an example, the thus derived zero-lift drag coefficients of both ascent and descent cases for a methane-fueled configuration are shown in Fig. 2.

2.4 Main propulsion rocket engines

The modeling of the engines and the derivation of the engine parameters such as specific impulse and T/W ratio and validation with existing engines are explained in-depth in [6].

The following Tables 1 and 2 summarize the resulting performance parameters used in this study.

For the landing burn of VTVL stages, the engines have to be throttled. The performance loss that occurs due to the reduced combustion chamber pressure necessary for throttling was not considered in the following trajectory optimization. As the landing burn only delivers a small amount of the overall Δv, it is expected that this impact is covered by the existing mass and performance margins.

2.5 Mass modeling

2.5.1 Structure

The structure mass was assessed with the DLR-SART tool *lsap* (Launcher Structure Analysis Program), which models the launcher structure as a beam. This allows the calculation of the global loads along the major structural components and the subsequent sizing of each segment to withstand the local loads. The global loads were evaluated on several load cases along the GTO trajectories. The load case of maximum product of dynamic pressure and Angle of Attack (AoA) had the biggest impact on the sizing of the structure. The analysis incorporated the change in effective AoA possible through steady winds and gusts. It was found that the loads during descent were not sizing for the main structures of the vehicles. While values such as the dynamic pressure or

Table 2 LOX/LCH4, LOX/LH2 rocket engine data

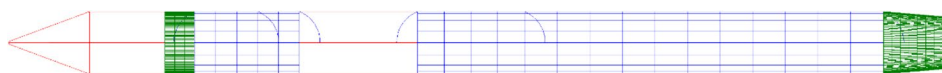| Propellants	LOX/LCH4				LOX/LH2			
Case	1st stage		2nd stage		1st stage		2nd stage	
Engine cycle	GG	SC	GG	SC	GG	SC	GG	SC
Expansion ratio	20	23	120	120	20	23	120	120
Sea level Isp [s]	289	314	–	–	366	394	–	–
Vacuum Isp [s]	320	343	348	366	406	428	440	459
Engine T/W [-]	105	77	85	71	98	75	82	70

Fig. 3 Exemplary visualization of structure model for a LOX/LH2 launcher, specifically the HH GG Med configuration

Fig. 4 Exemplary visualization of segment structure model for rear skirt of a LOX/LH2 launcher, specifically the HH GG Med configuration. Stiffener geometry and size are shown in 8:1 scale compared to the shell

scale stiffener/shell: 8:1
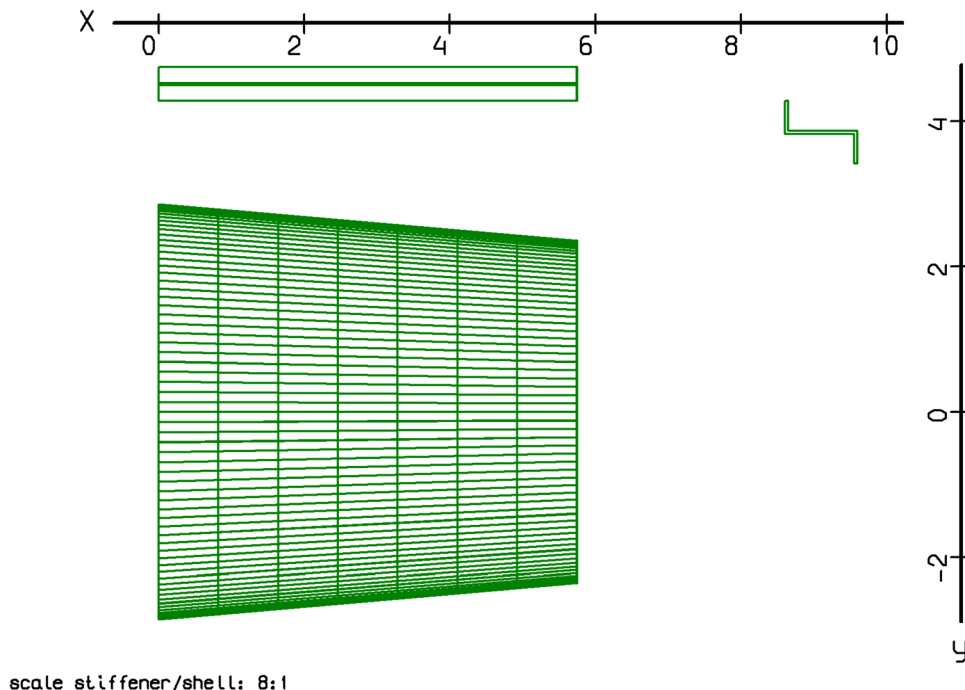
the axial or lateral acceleration might be higher during the descent, due to the reduced mass of the depleted stage, the actual loads within the structure are lower. This observation is further discussed in [14].

The fairing mass was not assessed with this tool, as the actual structural loads represent only one aspect that governs the fairing mass, and the others cannot be accurately assessed with this approach. Instead, the fairing mass was estimated by scaling the Ariane 5 fairing mass in proportion to surface area.

In the model, the interstage was represented as an Aluminum honeycomb structure, while other segments were depicted as conventional stringer/frame stiffened cylinders composed of AA 2219 alloy. An optimization process was applied to determine the precise number of stringers and frames for each segment, aiming to minimize total mass. The propellant tank's ullage pressure was set at 3 bar. A global safety factor of 1.25 was considered in the analysis, along additional margins for dynamic loads.

Figure 3 illustrates an example of the structural model. It depicts the stringer/frame stiffened propellant tanks in blue, the interstage and fairing in red, and the front and

Table 3 Design Matrix of ENTRAIN study with nomenclature abbreviations

Design parameter	Description	Nomenclature
Return method	**VTVL Downrange Landing**	**VL DRL**
	VTVL Return-to-Launch-Site	VL RTLS
	VTHL In-Air-Capturing	HL IAC
	VTHL Fly-Back	HL FB
Propellant	**LOx-LH2**	**H**
	LOx-LCH4	**C**
	LOx-LC3H8	**P**
	LOx-RP-1	**K**
Engine cycles	**Staged combustion**	**SC**
	Gas generator	**GG**
Upper stage Δv	**6.6 km/s**	**Hi**
	7.0 km/s	**Med**
	7.6 km/s	Lo

Options in bold are considered within this manuscript

rear skirts in green. A segment model for the rear skirt of a LOX/LH2 launcher is shown in Fig. 4 including the size and geometry of the optimized stiffener at 8:1 scale compared to the shell structure.

2.5.2 Propellant tanks and feedlines

The propellant system's modeling was conducted using the DLR-SART tool pmp (Propellant Management Program). This model includes the propellant tanks and incorporates the feed, fill, drain, and pressurization lines. The sizing of the hardware was determined through a simulation of the propellant and pressurization gas flow for the mission duration. This simulation facilitated the identification of the critical flow conditions within the lines, which then informed the sizing process.

A generic example of the propellant management system model for a LOX/LH2 launcher is shown in Fig. 5. The LOX tanks and feedlines are marked blue, the equivalent systems for LH2 market red. The pressurization lines are indicated in pink.

In addition to the usable propellant, a performance reserve of 0.9% and residuals of 0.36% were considered in the mass budget.

For all cryogenic propellants, an autogenous pressurization approach was assumed. Conversely, for the RP-1 tanks, helium pressurization was considered. Accordingly, the helium tanks required for this purpose were also sized and incorporated into the overall mass budget.

Cryogenic insulation of the propellant tanks was only considered for the LOX/LH2 launchers, for the hydrocarbon-fueled launchers no cryogenic insulation was included, following the example of the Falcon 9 with LOX/RP-1.

2.5.3 Recovery hardware

By definition the VTVL stages must include hardware that allows their safe and reliable return to earth, including a powered landing. While the engines are responsible for deceleration and control during propulsive phases, additional control surfaces are necessary for managing the vehicle's
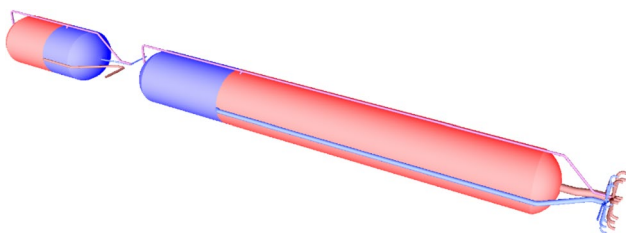

Fig. 5 Sketch of the model of propellant management system for both stages of a LOX/LH2 launcher, specifically the HH GG Med configuration

trajectory during non-propulsive descent phases within the atmosphere. These control surfaces also allow the returning stage to fly at small angles of attack. The lift and drag forces generated in this manner reduce the thermal loads on the stage, thereby allowing the reentry burn to be shorter. While different options exist for aerodynamic control surfaces (i.e., conventional fins would also be possible), for these study grid fins were chosen as the baseline design.

Alongside the control surfaces, landing legs are essential for the actual landing process. The mass of the recovery hardware in this study was estimated based on data from the Falcon 9. Although the exact values for Falcon 9 are not publicly available, their mass was estimated using in-house tools and reverse engineering techniques [15]. For the ENTRAIN RLV stages, the mass of the recovery hardware was estimated by linearly scaling the Falcon 9 recovery hardware mass in proportion to the dry mass of each stage.

In addition to the aforementioned recovery hardware, a thermal protection system is needed for the baseplate to protect the engine bay from the heat during reentry. A 2 cm thick layer of cork was chosen as a first guess, since there is little data available on the actual local heat loads. The generation of a comprehensive aerothermodynamic database would enable further optimization of this protective layer's thickness. It is presumed that the engine nozzle, which is designed to endure the thermal loads generated by the engine itself, is sufficiently robust to withstand the thermal stresses during reentry without the need for additional thermal protection.

2.5.4 Other subsystems/mass models

The mass model of the launchers was created using the SART tool stsm (Space Transport System Mass Estimation). This software applies empirical estimation formulas, which are grounded in historical data, to calculate the masses of various structural and subsystem elements. These elements include structural components such as the rear skirt, and subsystem masses such as engine equipment (including of engine controllers and wiring) as well as electrical systems including their harnesses. Other subsystems were sized based on the masses of corresponding components in the Ariane 6, including the power system and batteries, stage and fairing separation systems, avionics, the Reaction Control System (RCS), and the payload adapter.

Due to the inherently higher uncertainty in mass estimation for RLVs compared to ELVs, all first stage structures and subsystems were assigned a mass margin of 14%. The mass margin for the main engines for both stages was set at 12%. All other elements of the second stage were assigned a mass margin of 10%.
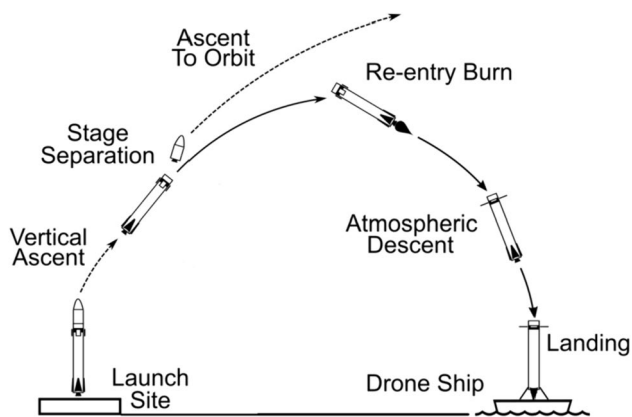
Fig. 6 Mission profile for downrange landing of first stage

2.6 Trajectory optimization

The mission profile for a mission including the recovery of the first stage via DRL is shown in Fig. 6. The assumptions used to optimize the ascent and descent phase are described in the following section. Due to constraints within the available trajectory optimization tools the two phases were optimized separately, however for the DRL mission type this approach yields sufficiently good results and agrees well with reverse-engineered trajectories from real vehicles [15]. Both ascent and descent trajectory optimizations were performed with the DLR tool *tosca*. It uses a direct single-shooting approach with a Runge–Kutta integration routine in combination with the optimization algorithm SLSQP [16]. For this type of performance assessment, the equations of motions are considered in three dimensions. The vehicle is modeled as point mass, no rotational dynamics are evaluated. The attitude of the vehicle is determined via the controls. The atmospheric model utilized in this study employs values of the NRLMSISE00 model [17] for Kourou.

2.6.1 Ascent

For the sizing of the launchers the performance into GTO was chosen, accordingly the ascent into a GTO with its perigee at 250 km was the reference ascent case. As CSG at Kourou in French Guyana was the designated launch location, the final GTO typically has an inclination of 6°.

To facilitate an efficient transfer of the payload into Geostationary Orbit (GEO), it is beneficial for the argument of perigee of the GTO to be approximately 0° or 180°, positioning it over the equator. To achieve this alignment, the upper stage is initially inserted into a 140×330 km parking orbit. It then raises its orbit to the final GTO configuration as it crosses the equator. This approach is necessitated by the relatively short burn time characteristic of the two-stage launchers, which would otherwise result in the Main Engine

Cut-Off (MECO) of the second stage occurring well before the stage reaches the vicinity of the equator.

This approach does have the drawback of requiring a second ignition of the second stage engine. However, given that the engines used in the second stage are identical to those in the first stage, the capability for reignition is inherently required. An additional consideration is the need to reserve some extra propellant for the chill-down of the engine prior to reignition. For this purpose, it was assumed that the mass flow equivalent to two seconds would be sufficient to adequately chill the engine for a successful reignition.

2.6.2 Descent

All launchers discussed hereafter use DRL on a barge (or some other landing platform in the Atlantic Ocean), to recover the first stage. As the barge can be freely positioned, no specific coordinates are targeted during optimization of the descent trajectory. The following landing conditions are targeted:

- Landing Flight Path Angle: $90° \pm 2°$
- Landing Velocity: 0 m/s–max. 2.5 m/s
- Landing Altitude: $0 \text{ m} \pm 10 \text{ m}$

In addition, the following constraints were imposed during the trajectory optimization:

- dynamic pressure of < 200 kPa
- estimated heat flux of < 200 kW/m^2 with respect to a (hypothetical) nose radius of 0.5 m
- lateral acceleration of < 3 g

These constraints were chosen based on trajectories reverse engineered from SpaceX' Falcon 9 flights [15]. The high dynamic pressure encountered during reentry, in comparison to the ascent phase, is considered non-problematic. This is because, during reentry, the stage is significantly lighter due to the expended fuel. As a result, the global axial forces and bending moments generated during this phase are still lower than those experienced during the maximum dynamic pressure phase of the ascent, as shown in [14].

For the trajectory the heat flux is estimated with the following modified Chapman equation:

$$\dot{q} = 20254.4 \, \text{W/cm}^2 \sqrt{\frac{\rho}{\rho_R} \frac{R_{N,r}}{R_N}} \left(\frac{v}{v_r}\right)^{3.05}$$

$R_{N,r}$ is reference nose radius (1 m), R_N is the vehicle nose radius (here 0.5 m for all vehicles), v is the vehicle's velocity and v_R is a reference velocity of 10000 m/s. In practice, the heat-flux constraint had the most impact on the Δv of the reentry boost.

As with the ascent, the descent trajectory optimization was also performed with the DLR tool *tosca*, with the optimization target being minimal propellant usage, while still respecting the above-mentioned constraints. For the entire trajectory the stage is simulated as a mass point without considering perturbations or rotational dynamics. While this approach is well suited to a performance estimation, it does not include the complexity of the control of the vehicle, especially during the reentry and landing phases.

3 Results

3.1 Nomenclature

The range of launchers considered in this study is categorized using a nomenclature that makes it easy to distinguish between vehicles based on key design space parameters, as outlined in Table 3. This nomenclature employs simple abbreviations for the return methods and engine cycles. In terms of propellants, each propellant combination is represented by a unique substitute letter. The first stage separation velocity is indicated by terms like "Hi" for high, "Med" for medium, and "Lo" for low separation velocity.

For example, a launcher featuring vertical landing with downrange landing, LOX/LH2 in both stages, gas generator engines and an upper stage Δv of 7.0 km/s would be dubbed: *VL DRL HH GG Med.* As this paper only discusses the VTVL stages, the "VL DRL" part is superfluous and is omitted in the following discussions.

3.2 Overview

Based on the assumptions and boundary conditions described in sect. 1.1 and the methods outlined in sect. 2, the propellant loading of the launchers was systematically varied. This iterative process continued until a viable solution was identified that aligned with the specific combination of upper stage Δv, fuel type and engine cycle being targeted. The key characteristics of the resulting launchers are given in Table 4. Not all possible combinations were investigated. For the reasons given in sect. 1.1 the RTLS return method and the upper stage Δv 0f 6.2 km/s and 7.6 km/s were discontinued. Also, the denser hydrocarbons, RP-1 and LC3H8, were only investigated for gas generator engines.

The following sections give an overview over the results with regard to geometry, mass, SI and inert mass ratio as well as the ascent and descent trajectories. The impact of the individual design degrees of freedom is discussed in sect. 4.

3.3 Size and geometry

Figure 7 presents a sketch illustrating the geometries of the resulting launchers from the study. A notable observation from this figure is that the launchers fueled by LCH4 are the largest in size, even surpassing their hydrogen-fueled counterparts significantly. Despite LCH4 having a higher density compared to hydrogen, the volume of these launchers is larger due to the substantially greater propellant loading required for LCH4. The difference in mass between the hydrogen and hydrocarbon-fueled launchers are explored in more detail in sect. 3.4.

Given the specified T/W at liftoff, it is observed that accommodating the engines beneath the stage becomes a challenge for the hydrocarbon-fueled launchers. In certain designs, this constraint leads to some engine nozzles slightly extending beyond the diameter of the fuselage. This issue is not encountered with the hydrogen-fueled launchers, primarily due to hydrogen's lower density, which allows for more spacious engine arrangement within the confines of the fuselage dimensions.

Generally, it is expected that this issue also stems from the sheer size of the launchers, since the base plate area does not increase linearly with the vehicle mass, which in turn is proportional to the thrust.

3.4 Mass

The Gross Lift-Off Mass (GLOM) of each configuration is shown in Fig. 8. At first sight, the difference between the hydrogen and hydrocarbon-fueled launchers is clearly apparent. This is expected due to the lower specific impulse of hydrocarbon-fueled stages.

Figure 9 shows the dry mass of the investigated launchers. The difference between hydrocarbon and hydrogen-fueled launchers is still significant but smaller than when only considering the GLOM. Within the hydrocarbon variants it is noteworthy that while the hydrocarbon-fueled launchers (for the same upper stage Δv) all exhibit similar GLOM, for the dry mass differences appear, favoring the denser hydrocarbons over the less dense LCH4.

The dry mass of the reusable first stages, with a particular focus on the portion comprised of the propulsion subsystem, is depicted in Fig. 10

3.5 Dimensionless parameters

To evaluate the performance of rocket stages, dimensionless parameters can be utilized. In the forthcoming paragraph, two such parameters will be used: The Structural Index (SI) excluding engine mass, and the Inert Mass Ratio (IMR). These parameters are defined as follows:

Table 4 Key parameters of investigated VTVL launchers

Fuel	LH2			LCH4			LC3H8	RP-1		Hybrid
Engine cycle	GG	GG	SC	GG	GG	SC	GG	GG	GG	GG
2nd stage Δv [km/s]	6.6	7.0	7.0	6.6	7.0	7.0	6.6	6.6	7.0	7.0
Staging category	Hi	Med	Med	Hi	Med	Med	Hi	Hi	Med	Med
Designation	HH GG Hi	HH GG Med	HH SC Med	CC GG Hi	CC GG Med	CC SC Med	PP GG Hi	KK GG Hi	KK GG Med	CH GG Med
1st stage										
Propellant loading [t]	392	311	250	1193	865	637	1251	1221	899	441
Total dry mass [t]	47.9	41.7	35.9	98.1	73.2	57.3	94.2	88.4	68.1	41.2
Propulsion mass [t]	9.1	8	8.4	23.9	18.4	19	23.1	22.8	18	9.4
No. of engines [-]	9	9	9	17	15	11	15	15	13	9
Single Engine Thrust (sea level) [kN]	782	689	561	1165	1021	1062	1350	1352	1234	864
2nd stage										
Propellant loading [t]	63.8	77.7	66.3	125.6	151.8	128.7	137.2	135.9	169.2	72.1
Dry mass [t]	8.2	8.4	7.4	10.1	9.8	9.2	10.2	10	9.8	7.8
Propulsion mass [t]	1.3	1.2	1.1	1.9	1.6	2	2.1	2.1	1.9	1.1
Engine Thrust (vacuum) [kN]	942	829	652	1407	1229	1238	1629	1637	1495	777
Total Launcher										
Height [m]	86.5	79.9	75.1	91.3	83.6	76.2	88.9	82.8	77.3	69.7
Diameter [m]	5.4	5.3	5	6.1	5.7	5.1	5.9	5.8	5.4	5.0
Payload to GTO [t]	7.4	7.49	7.46	7.42	7.45	7.62	7.4	7.55	7.64	7.47
GLOM [t]	519	447	367	1434	1107	840	1500	1463	1153	570

Fig. 7 Sketch of investigated configurations with a VTVL first stage. Numbers above fairing indicate the staging via upper stage Δv
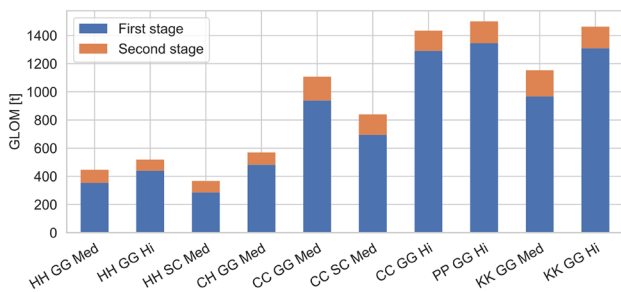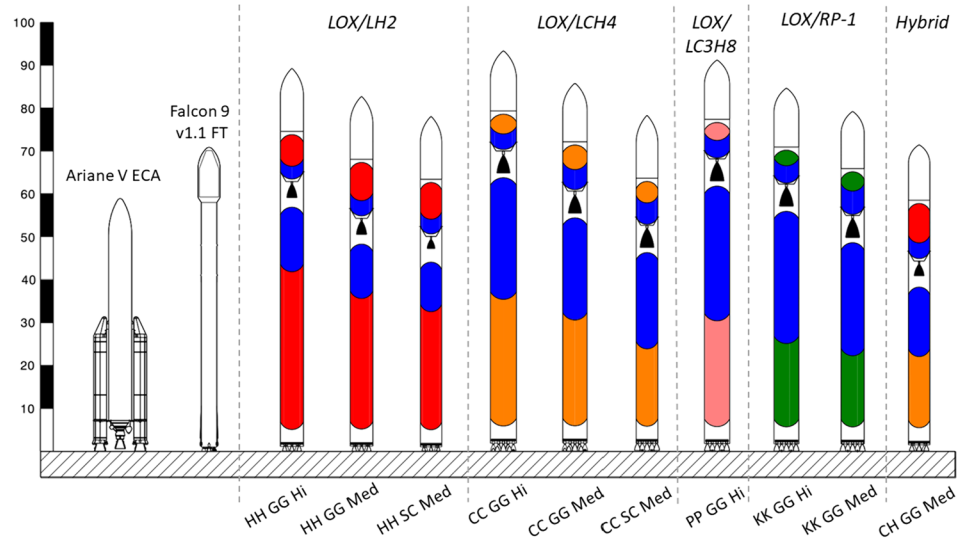

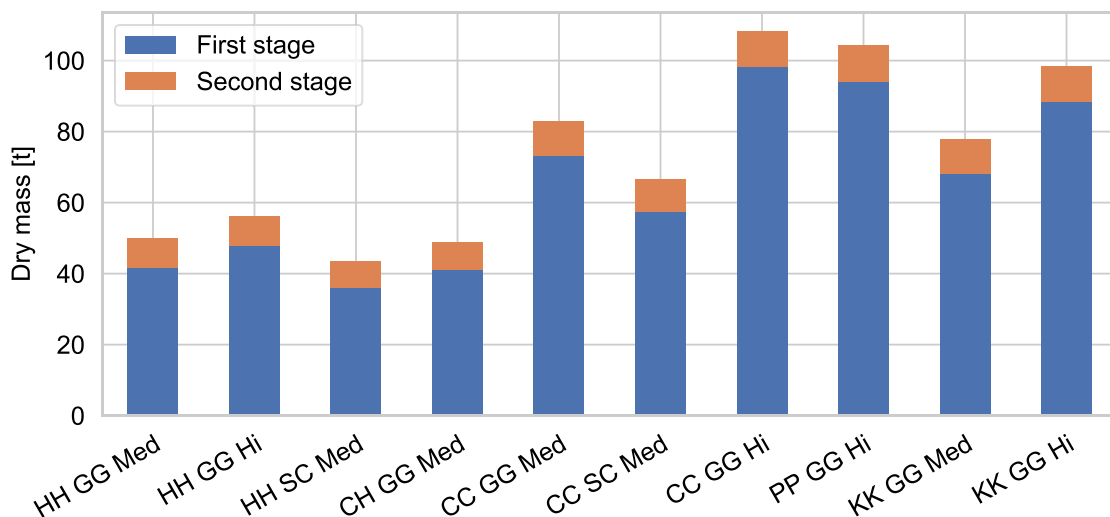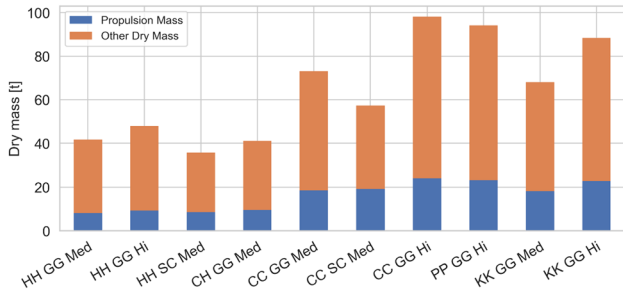**Fig. 8** GLOM of configurations with VTVL first stages with different propellant combination, staging velocities and engine cycles

$$\text{Structural index (SI)} = \frac{m_{\text{dry}} - m_{\text{engines}}}{m_{\text{propellant}}}$$

$$\text{Inert mass ratio (IMR)} = \frac{\text{GLOM}_{\text{stage}} - m_{\text{ascent propellant}}}{\text{GLOM}_{\text{stage}}}$$

While similar, the IMR is a better indicator of the ascent performance of the stage, since the descent propellant is essentially inert ballast during that phase. The SI is a good indicator of the overall efficiency of the stage design with regard to its dry mass.

Figure 11 shows the SI and IMR for all investigated reusable first stages as well as the Falcon 9. The comparison of the Falcon 9 to the launchers of this study is discussed in sect. 4.5.

The hydrocarbon stages have significantly lower SI's than hydrogen stages, mostly due to low density of LH2.

Fig. 9 Dry Mass of configurations with VTVL first stages with different propellant combination, staging velocities, and engine cycles

Fig. 10 Dry Mass of configurations with VTVL first stages with different propellant combinations, staging velocities and engine cycles, with the portion attributable to the propulsion subsystem highlighted

Fig. 12 Illustration of propulsive maneuvers in reentry profile (altitude over time)

This is also true for the IMR, yet the difference appears reduced. The reduced disparity in IMR is primarily due to the increased requirement for descent propellant in hydrocarbon stages, which is a consequence of their lower engine efficiency. This additional propellant requirement partially offsets the benefits gained from having a lower SI.

The effect of the staging velocity can also be seen in these values. For launchers that have a lower upper stage Δv and consequently are the largest within their respective propellant group, there is a more significant disparity between the SI and IMR. This greater difference arises from the increased need for descent propellant in these stages with higher separation velocities. The additional propellant is required to decelerate the stage adequately, ensuring it does not exceed the heat-flux constraints during descent.

3.6 Trajectories

By their very nature, the ascent and descent trajectories contain many aspects that are of interest for the launch system, showing the evolution of all parameters is beyond the scope of this paper. In the context of this study the trajectories

primarily serve as a tool for determining the final sizing of the launchers. Therefore, the focus in this section will be on the return trajectory, as it represents the critical and novel element in these partially reusable launch concepts.

Two exemplary reentry profiles are illustrated in Fig. 12 with indication of the reentry and landing burns. These are characterized by sharp changes in the profile when the engines are ignited or extinguished. The two aforementioned constraints (200 kW/m^2 and 200 kPa) are indicated as well. It can be seen that the heat-flux constraint is the sizing constraint for this type of downrange reentry.

The ascent and descent during the ballistic arch after stage separation, but before the reentry burn, coincide in this perspective on the right edge of the figure.

Figure 13 illustrates the reentry profile (altitude over velocity) for all stages. It is observed that all stages exhibit a similar reentry trajectory, which aligns with expectations since the trajectory optimizer is designed to avoid regions of

Fig. 11 Structural Index and inert mass ratios over propellant mass of reusable VTVL first stages for different propellant combinations

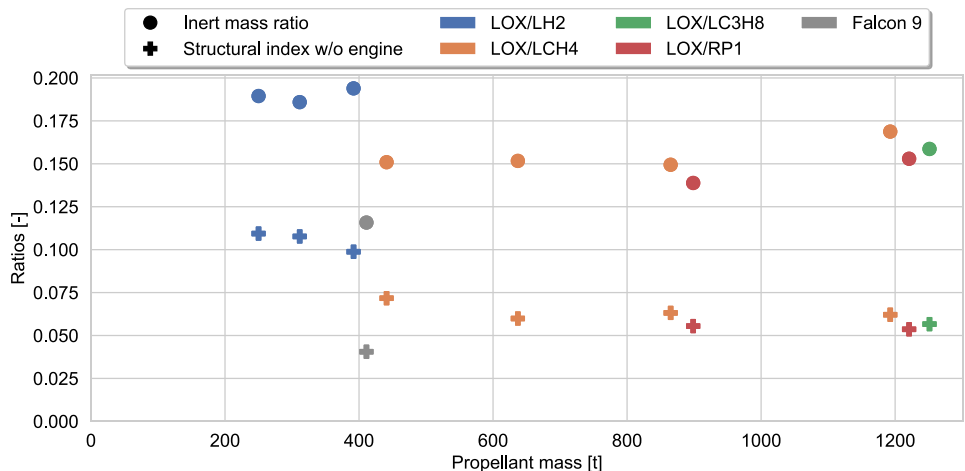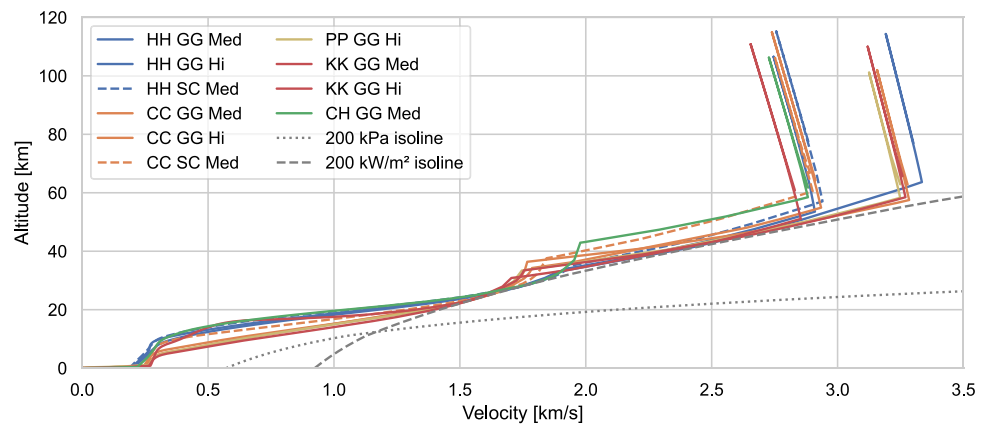**Fig. 13** Reentry profile of reusable VTVL first stages including the constraints for heat flux and dynamic pressure

high thermal loads while maximizing deceleration through aerodynamic forces. The clustering in the graph represents the two different staging velocities. The slight differences in initial conditions arise from variances in the ascent trajectory, as well as iteration limits applied with regard the upper stage Δv. Despite these initial discrepancies, the stages exhibit remarkably similar behavior post-reentry burn. The primary differentiator at this stage is the type of propellant used.

It can be seen that hydrogen stages are decelerated to ~1.9 km/s, whereas the hydrocarbon-fueled stages employ their engines to decelerate to ~1.75 km/s. Despite this difference in speeds at the end of the reentry burn, the maximum heat loads experienced by both types of stages are identical. The lower ballistic coefficient of the hydrogen stages enables them to achieve more deceleration through aerodynamic

means while still respecting the constraint set for maximum heat flux.

This difference is further illuminated when the cumulative forces acting on the returning stages over the entirety of the return trajectory are examined. Figure 14 presents these results for all evaluated stages. As anticipated, higher staging velocities necessitate additional engine Δv for deceleration during the reentry burn. A comparison between hydrogen and hydrocarbon-fueled stages reveals a greater impact of aerodynamic forces on the trajectory of hydrogen stages. Even near depletion the ballistic coefficient of the hydrogen stages is lower, which results in increased aerodynamic deceleration. Consequently, the engines of hydrogen-fueled stages are required to provide less Δv for both reentry and landing burns. Overall, this effect amounts to approximately 0.25 km/s less in
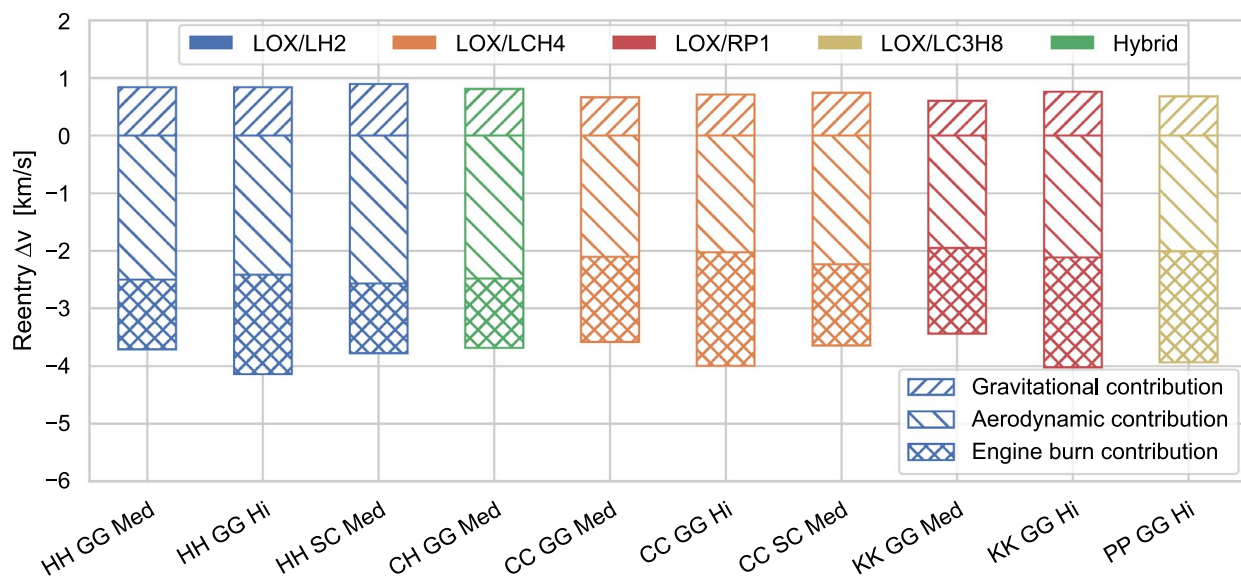

Fig. 14 Reentry velocity changes integrated of descent trajectory for returning VTVL stages

propulsive Δv. As a side effect of the decreased ballistic coefficient, the flight of the hydrogen-fueled stages has a longer duration, leading to slightly larger gravitational acceleration. This does not affect the propulsive budget, as it is compensated by a larger aerodynamic contribution as well.

The first stage of the hybrid launcher displays an unexpected behavior; despite being fueled with methane, it appears to follow the trends typically associated with hydrogen-fueled stages, as indicated in Figs. 13 and 14. This phenomenon can be attributed to two factors: First, the hydrogen upper stage is lighter than the equivalent methane upper stage, leading to less loads and thus potentially lighter structures. Second, due to the lighter upper stage the first stage itself also has a much smaller propellant loading (441 t) compared to the propellant loadings of the other methane stages (865 t). Assuming a similar SI, it is reasonable to infer that the dry mass of a stage is directly proportional to its volume. Meanwhile, the aerodynamic forces acting on the stage scale linearly with its cross-sectional area. This relationship results in heavier vehicles having higher ballistic coefficients, an example of the effects of the square–cube law. These two effects together lead to the first stage of the hybrid launcher having a reentry profile more similar to the hydrogen-fueled stages than the purely methane-fueled cases.

4 Discussion

As with every study, these results have to be seen in context with the underlying requirements and assumptions. The chosen reference orbit and the requirement of propulsively landing the first stage lead to considerable Δv needs. This, coupled with the TSTO architecture, leads to designs where each individual stage has to provide a substantial amount of Δv. Consequently, in this case, the specific impulse of the engines has an especially large impact on the overall vehicle size and mass, favoring solutions with higher specific impulses such as utilizing hydrogen as fuel or opting for staged combustion engines. For a lower energy reference orbit the comparison would yield different results, likely shifted toward the design choices with lower specific impulse. For now, the ability to lift significant payload mass into GTO remains a relevant for European launchers, but this might change if in-space tug services become economically viable or if the GTO market ceases to be relevant.

The subsequent sect. 4.1 delves into the comparison metrics for the various design options. Sections 4.2–4.4 each concentrate on a major design variable: fuel type, engine cycle, and staging velocity, respectively. Section 4.5 presents a comparison between the KK GG Med launcher and the

Falcon 9. Finally, in sect. 4.6 the limitations of the study are discussed.

4.1 Metrics of comparison

The primary objective of most contemporary launcher development programs, beyond simply ensuring access to space, is to reduce the cost of transporting payloads into orbit. This drive for cost reduction serves as the principal motivation behind the development of reusable stages. Thus, it is logical that the core metric of comparison should be the cost of the individual systems. However, cost estimation for launcher systems, even for ELV, remains an imprecise field, with a plethora of examples of programs exceeding their estimated costs. For RLV stages this is especially challenging, since no experience with the operation and refurbishment of these type of stages exists within Europe.

To navigate around these significant uncertainties, the upcoming sections will concentrate on GLOM and dry mass as comparison metrics. Of these two, the dry mass is considered a better indicator of the actual cost since the GLOM is dominated by the propellant mass. In the case of liquid propellant stages, the cost of the propellant typically constitutes only a small fraction of the total expenses.

While the dry mass is an imperfect surrogate, it should be noted that well-established cost estimation tools such as TRANSCOST rely on the dry mass to estimate the cost. Even more granular cost estimations methods that employ bottom-up approach usually estimate the cost of individual components based on their dry mass. In cases where the differences in dry mass are marginal, the final outcome of a cost comparison remains uncertain. However, in cases where there are significant disparities in the dry mass of the systems being compared, it is reasonable to anticipate that the cost comparison will yield a similar outcome.

4.2 Impact of fuel

For a more in-depth illustration of the impact of the fuel choice on the launcher mass, Figs. 15 and 16 shows the GLOM and dry mass for the launchers using gas generator cycle engines and an upper stage Δv of 6.6 km/s, since launchers with all investigated-fuel types were examined for this staging velocity.

For both GLOM and dry mass, the disparity between hydrogen and hydrocarbon fuels is significantly more pronounced than the differences among the various hydrocarbons, particularly in terms of GLOM. When it comes to dry mass, although the difference is less marked, it remains substantial. With respect to GLOM, the variances between the hydrocarbon fuels are relatively minor, yet in terms of dry mass, the denser hydrocarbons result in a noticeably lower mass. Notably, even though methane possesses the highest
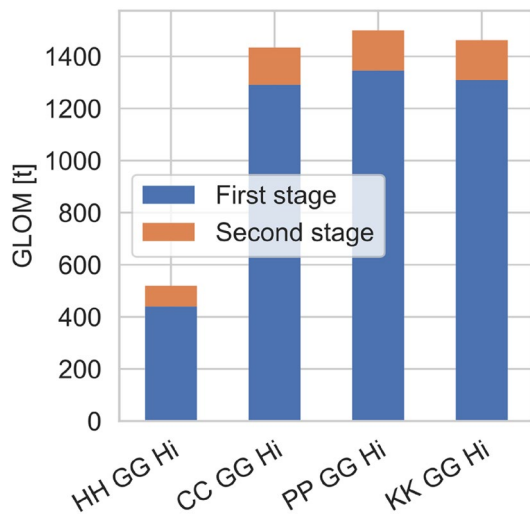
Fig. 15 GLOM of configurations with high separation velocity and gas generator cycle engines
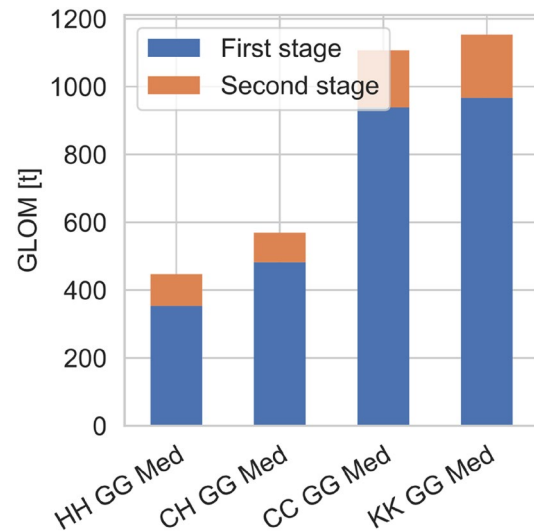

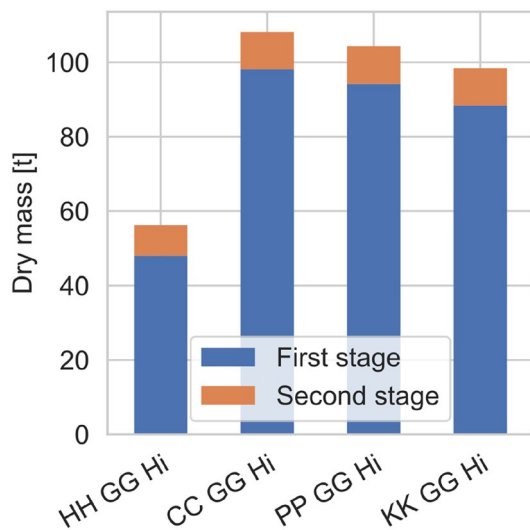**Fig. 17** GLOM of configurations with medium separation velocity and gas generator cycle engines

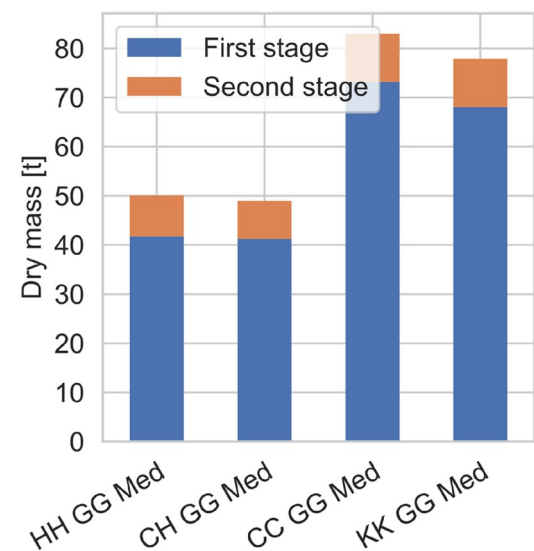**Fig. 16** Dry mass of configurations with high separation velocity and gas generator cycle engines

Fig. 18 Dry mass of configurations with medium separation velocity and gas generator cycle engines

specific impulse among the hydrocarbons examined in this study (see Tables 1 and 2 and [6]), its utilization as a fuel leads to the highest dry mass, almost twice the dry mass of the equivalent hydrogen-fueled launcher.

In the instances where the upper stage Δv is 7.0 km/s, as depicted in Figs. 17 and 18, the comparison between methane and hydrogen-fueled versions shows a slightly improved scenario. However, the dry mass of the reusable first stage of the methane-fueled launchers is still 76% heavier compared to their hydrogen-fueled counterparts. The primary contributor to this significant difference is the greater mass of the propulsion system in methane-fueled launchers, shown in Fig. 10, which in this case is 130% heavier

than the hydrogen-fueled counterpart. Although methane engines offer higher T/W ratios, the increased propellant load required for methane-fueled launchers leads to substantially higher thrust demands. This, in turn, results in a greater propulsion mass.

The hybrid launcher configuration, featuring a methane-fueled lower stage and a hydrogen-fueled upper stage, demonstrates the lowest dry mass among all configurations with gas generator engines. However, its GLOM is higher compared to an equivalent all-hydrogen stage. It is also important to consider that the hybrid launcher required two
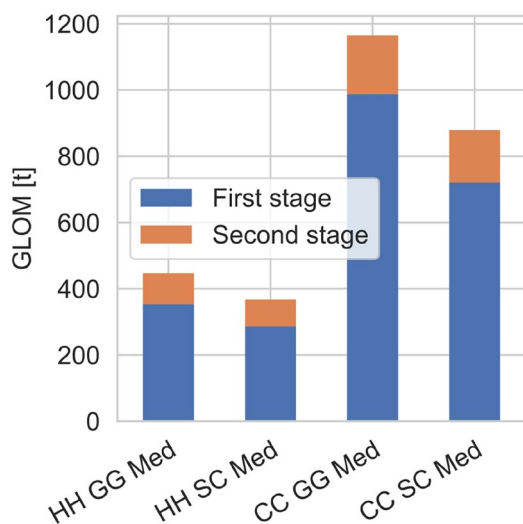
Fig. 19 GLOM of configurations with staged combustion cycle engines and counterparts with gas generator engines
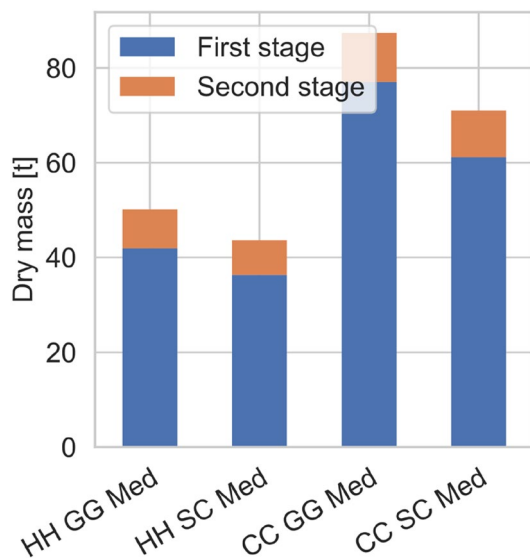

Fig. 20 Dry mass of configurations with staged combustion cycle engines and counterparts with gas generator engines

distinct rocket engines, one for each fuel. This is likely to increase development costs due to the complexities involved in designing, testing, and manufacturing two different propulsion systems.

4.3 Impact of engine cycle

Within this study two engine cycles were considered: gas generator and staged combustion. Historically, these are the two most common engine types for main rocket engines of orbital vehicles. An in-depth discussion of the assumptions for both cycles and their modeling can be found in [6].

In the following Fig. 19 and Fig. 20, the two launchers modeled with staged combustion engines are presented alongside their counterparts equipped with gas generator cycle engines. One of these launchers is fueled with hydrogen, while the other uses methane. As expected, the launchers with the closed engine cycles can fulfill the required mission with substantially less GLOM and dry mass. The difference is especially pronounced for the methane-fueled version. For the hydrogen-fueled launchers, those utilizing gas generator engines have a 22% higher GLOM compared to their counterparts with staged combustion engines. In the case of methane-fueled launchers, this difference increases to 32%. Regarding the dry mass of the reusable first stage, the hydrogen and methane variants show a difference of 16 and 27%, respectively, when comparing gas generator engines to staged combustion engines.

4.4 Impact of staging velocity

As previously discussed in sect. 1.1, only the high and medium separation velocities are included herein. The more extreme separation velocities, coinciding with upper stage Δv of 6.2 and 7.6 km/s, resulted in excessively large vehicles, especially for the hydrocarbons. Of the two remaining staging velocities, the medium separation velocities deliver lower GLOM and dry mass across all propellants, as can be seen in Fig. 8. It should be noted that with the higher staging velocity the reusable fraction of the launcher increases and thus that a cost-optimal staging will not necessarily coincide with the lowest mass optimum.

In contrast to VTHL return methods, the loads during reentry do not differ significantly between the different staging velocities. The reentry burn is optimized so that the same heat-flux constraints are respected. Consequently, higher separation velocities lead to higher Δv requirements for the descent and thus larger descent propellant masses.

4.5 Comparison with Falcon 9

Currently only one orbital launch vehicle with a reusable VTVL first stage is in operation, the Falcon 9. To assess the Falcon 9, the launcher was reverse-engineered on system level with publicly available data [15] with the tools described in chapter 3. The results from this reverse engineering have informed the methodology used to assess the VTVL stages within this study. The resulting values for the performance and mass of the Falcon 9 are in good agreement with the publicly available data including the broadcast of the trajectory. This indicates that the methodology described in chapter 3 is suited to the modeling of this type of vehicles.

In Figs. 21 and 22 the GLOM and the SI data of the Falcon 9 are shown compared to the KK GG Med configuration investigated within this study.
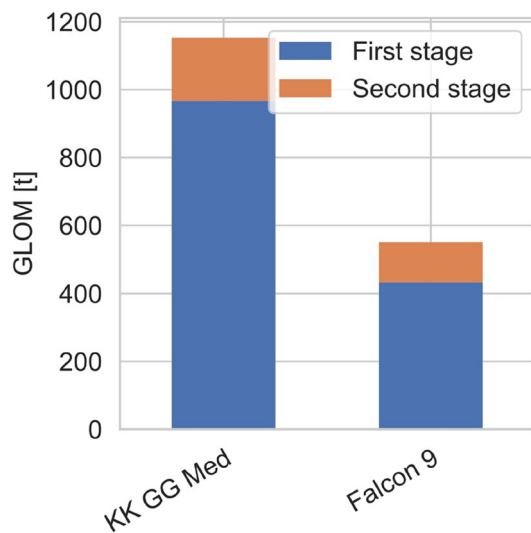
Fig. 21 GLOM comparison of the configuration KK GG Med with the Falcon 9
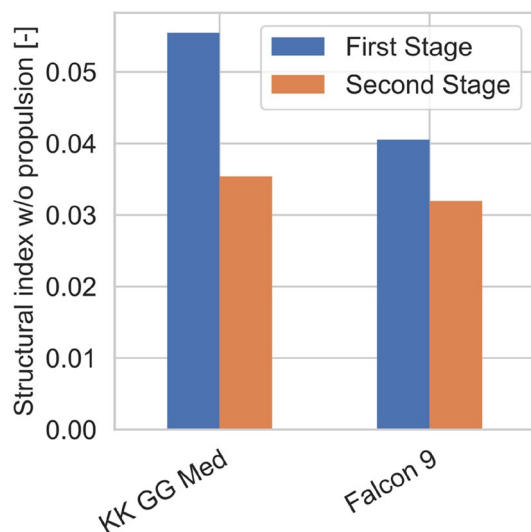

Fig. 22 Dry mass comparison of the configuration KK GG Med with the Falcon 9

At first glance, it becomes clear that the KK GG Med launcher is significantly larger and heavier than the Falcon 9. This is partially explained by the different payload performance into GTO while recovering the first stage on a barge (7.5t for the ENTRAIN launcher vs. ~5.5t for the Falcon 9). However, this difference accounts only for ~36% difference, while the total mass of the ENTRAIN launcher is more than twice the weight of the Falcon 9.

One major difference is found in the T/W of the engines. While the gas generator kerosene engine used in the first stage of the KK GG Med configuration have a T/W of 105, for the Merlin 1D a value of ~160 was assumed for the Falcon 9 reverse engineering. As the performance with regard to specific impulse is similar, discussed in [6], the difference in T/W is almost entirely caused by differences in the estimated mass of the engines.

But even in the SI without the propulsion subsystems, shown in Fig. 22, differences between the two stages can be found. For both stages the ENTRAIN launcher has higher SI values than the Falcon 9. This difference is only compounded by the fact that the propellant loading of the Falcon 9 is significantly lower (411t vs 899t in the first stage) and thus the SI should be higher. Figure 11 shows the SI and the IMR over the propellant mass, where this factor is clearly apparent.

The underlying cause can be found in the design of the stages themselves. While on the surface the launchers share many characteristics, the Falcon 9 includes features that significantly lower the dry mass. Most importantly, the use of highly subcooled and thus densified propellants as well as the use of aluminum–lithium for the main structural elements.

This crosscheck with values reverse engineered from the Falcon 9 indicates that the launchers derived within this study are realistic and feasible. However, the challenge of actually achieving these values in a concrete design should not be underestimated, even if they are not as ambitious as the metrics of the Falcon 9.

4.6 Limitations

Any comparison of design options for launch vehicles (or any technical system) represents a compromise between the depth of the analysis, the breadth of scope and the available resources. To assess the effect of high-level design choices, such as propellant combination, engine cycle or staging velocity, the breadth of this study is necessarily large. While we believe sufficient depth was achieved to characterize the performance of the vehicles and their main subsystems, many details of an actual implementation were not directly evaluated.

In general, the uncertainties in the performance assessment are smaller than the uncertainties in the mass assessment. For a given mass budget the trajectory integration can be done precisely, with the main uncertainties lying in the propulsion performance and the aerodynamic properties. As discussed in [6], the propulsion datasets are cross-checked with existing engines where possible. With regard to the ascent aerodynamics, the engineering methods used are adapted to the typical ascent configuration and the impact on the overall performance is small. The largest uncertainty with regard to the performance assessment lies in

the aerodynamic properties during descent. The complex geometry resulting from flying engine first cannot be easily modeled with engineering approaches. While the chosen approach, described in sect. 2.3, is corroborated by wind tunnel and a-posteriori CFD results, the fact remains that no experience in flying this type of vehicle exists in Europe and thus some uncertainty is unavoidable with regard to the aerodynamic properties in engine-forward flight.

The larger uncertainties of the chosen methodology lie in the dry mass estimation of the launchers, especially for the reusable first stages. The mass estimations mostly rely on empirical relations based on historical data or conceptual design tools that cannot depict the full complexity of an actual launch vehicle. While the general suitability of the methodology is affirmed by its ability to replicate the Falcon 9, as discussed in sect 4.5, uncertainties remain with regard to an actual European implementation of such a vehicle.

Nonetheless, more detailed investigations of reduced scope but increased technical depth, performed within the scope of ENTRAIN2 for the hybrid launcher, essentially confirmed the results and did not identify any major inconsistencies [13, 18, 19].

On a broader scope, the chosen metrics of comparison, as discussed in the precious sections, don't account for all economical or operational aspects of the investigated design options. For example, the refurbishment or recovery effort per mass might vary depending on the staging velocity or propellant choice. However, even with this caveat, the assessment of the vehicle mass and performance is a necessary part of the full picture and essential in avoiding design choices that are optimal for a given aspect/subsystem without an understanding of the impact on the system level.

Finally, the launchers shown herein are not the result of a full multidisciplinary optimization. As discussed in sect. 1.1, the staging is varied parametrically and for many secondary parameters (for example the engine nozzle expansion ratio) are chosen based on previous experience or expert judgements. While this is sufficient to arrive at representative vehicle designs, it leaves some potential for optimization and might introduce some distortions into the comparison.

5 Conclusion

Within this paper ten different launchers, with a reusable VTVL first stage, were preliminarily sized using different assumptions for staging, fuel choice and engine cycle to achieve a payload performance of 7.5t into GTO. For all stages a reusable first stage, recovered via downrange landing, was assessed. For each launcher dedicated technical models for the major subsystem were generated, including structure, propulsion, propellant tanks, feed-, fill- and pressurization lines as well as aerodynamics datasets for ascent and descent. The performance was assessed via trajectory optimization for both ascent and descent.

This effort lead to realistic and quantified data with regard to the effect of the investigated design options for a European reusable first stage which can serve as a technical foundation in discussions with regard to future European launchers.

The high Δv required to fulfill a GTO mission while also safely decelerating the reusable stage during reentry leads to substantial launcher sizes, especially for the hydrocarbon-fueled launchers, where the lower specific impulse has a large impact on the overall launcher mass even with the lower structural indexes. The methane-fueled VTVL stages exhibited a 76% higher dry mass than their hydrogen-fueled equivalents. With regard to GLOM, the entirely methane-fueled launcher with gas generator engines is almost two and a half times as heavy as its hydrogen counterpart.

Within the investigated hydrocarbons (RP-1, propane and methane), the RP-1 fueled cases result in the smallest and lowest dry mass launch vehicles. The GLOM of all vehicles fueled by hydrocarbons was fairly similar.

As expected, using staged combustion engines leads to noticeably reduced launcher sizes and masses. The dry mass of the reusable first stage for hydrogen and methane-fueled configurations is reduced by 14 and 22% respectively, compared to equivalent launchers with gas generator engines.

The use of methane (or likely any hydrocarbon) in the first stage with a hydrogen-fueled upper stage leads to a significantly lighter launcher than the use of methane in both stages. This hybrid configuration even has a slightly smaller dry mass than the entirely hydrogen-fueled version. However, this necessitates the development of two separate rocket engines for each fuel, and the handling of two different fuels on the launch pad.

Declarations

References

1. Dominguez Calabuig, G.J., Wilken, J.: Pre-conceptual staging trade-offs of reusable launch vehicles. 9th European Conference for aeronautics and space science, EUCASS 2022 (2022)
2. Dresia, K., et al.: Multidisciplinary design optimization of reusable launch vehicles for different propellants and objectives. J. Spacecr. Rocket. **58**(4), 1017–1029 (2021)
3. Marwege, A., Gülhan, A., Klevanski, J., et al.: RETALT: review of technologies and overview of design changes. CEAS Space J. **14**, 433–445 (2022). https://doi.org/10.1007/s12567-022-00458-9
4. Kuczera, H., Johnson, C.: The major results of the FESTIP system study. 9th International Space Planes and Hypersonic Systems and Technologies Conference (1999)
5. Dietlein, I., et al.: Overview of system study on recovery methods for reusable first stages of future European launchers, CEAS space journal, Submitted for publication (2024)
6. Sippel, M., Wilken, J.: Selection of propulsion characteristics for systematic assessment of future European RLV-options, CEAS space journal, Submitted for publication (2024)
7. Bussler, L., et al.: Comparative analysis of European horizontal-landing reusable first stage concepts, CEAS space journal, Submitted for publication (2024)
8. Stappert, S., et al.: Options for future European reusable booster stages: evaluation and comparison of VTHL and VTVL return methods, CEAS space journal, Submitted for publication (2024)
9. Stappert, S., Wilken, J., Sippel, M.: Evaluation of European Reusable VTVL Booster Stages. 2018 AIAA SPACE and astronautics forum and exposition. https://elib.dlr.de/121912/ (2018)
10. Vukelich, S.R., Stoy, S.L., Burns, K.A., et al.: Missile DATCOM, volume I-final report, McDonnel Douglas, Technical report AFWAL-TR-86-3091
11. Klevanski, J., Sippel, M.: Beschreibung des Programms zur aerodynamischen Voranalyse CAC Version 2 (2003)
12. Nichols James, O., Edward, A.N.: Aerodynamic characteristics of blunt bodies. No. NASA-CR-59914 (1964)
13. Stappert, S., et al.: European next reusable ariane (ENTRAIN): a multidisciplinary study on a VTVL and a VTHL Booster Stage. In: Proceedings of the International Astronautical Congress, IAC (2019)
14. Sippel, M., Stappert, S., Bussler, L.: Systematic assessment of a reusable first-stage return options, IAC-17-D2.4.4, 68th International Astronautical Congress, Adelaide, Australia, http://elib.dlr.de/114960/ (2017)
15. Stappert, S., Sippel, M.: Critical analysis of spaceX falcon 9 v1.2 launcher and missions, SART TN-009/2017 (2017)
16. Kraft, D., Schnepper, K.: SLSQP—a nonlinear programming method with quadratic programming subproblems. DLR, oberpfaffenhofen 545 (1989)
17. Picone, J.M., et al.: NRLMSISE-00 empirical model of the atmosphere: Statistical comparisons and scientific issues. J. Geophys. Res. Space Physics (2002). https://doi.org/10.1029/2002JA009430
18. Wilken, J., Stappert, S.: Investigation of a European reusable VTVL first stage. 8th European Conference for aeronautics and space sciences (EUCASS), Madrid, Spain. https://elib.dlr.de/135409// (2019)
19. Wilken, J., et al.: Multidisciplinary design analysis of reusable European VTHL and VTVL Booster Stages. 2nd International Conference on High-Speed Vehicle Science Technology (HiSST), 11–15 September 2022, Bruges, Belgium